Brief Communication

MOLECULAR METABOLISM

Inducible overexpression of adiponectin receptors highlight the roles of adiponectin-induced ceramidase signaling in lipid and glucose homeostasis

William L. Holland [1,*,4], Jonathan Y. Xia [1,4], Joshua A. Johnson [1], Kai Sun [2], Mackenzie J. Pearson [1], Ankit X. Sharma [1], Ezekiel Quittner-Strom [1], Trevor S. Tippetts [1], Ruth Gordillo [1], Philipp E. Scherer [1,3]

ABSTRACT

Objective: Adiponectin and the signaling induced by its cognate receptors, AdipoR1 and AdipoR2, have garnered attention for their ability to promote insulin sensitivity and oppose steatosis. Activation of these receptors promotes the deacylation of ceramide, a lipid metabolite that appears to play a causal role in impairing insulin signaling.

Methods: Here, we have developed transgenic mice that overexpress AdipoR1 or AdipoR2 under the inducible control of a tetracycline response element. These represent the first inducible genetic models that acutely manipulate adiponectin receptor signaling in adult mouse tissues, which allows us to directly assess AdipoR signaling on glucose and lipid metabolism.

Results: Overexpression of either adiponectin receptor isoform in the adipocyte or hepatocyte is sufficient to enhance ceramidase activity, whole body glucose metabolism, and hepatic insulin sensitivity, while opposing hepatic steatosis. Importantly, metabolic improvements fail to occur in an adiponectin knockout background. When challenged with a leptin-deficient genetic model of type 2 diabetes, AdipoR2 expression in adipose or liver is sufficient to reverse hyperglycemia and glucose intolerance.

Conclusion: These observations reveal that adiponectin is critical for AdipoR-induced ceramidase activation which enhances hepatic glucose and lipid metabolism via rapidly acting "cross-talk" between liver and adipose tissue sphingolipids.

© 2017 Published by Elsevier GmbH. This is an open access article under the CC BY-NC-ND license (http://creativecommons.org/licenses/by-nc-nd/4.0/).

Keywords Sphingolipid; Insulin resistance; NAFLD

1. INTRODUCTION

The discovery of adipocyte-specific secreted molecules, termed adipokines, has dispelled the notion of adipose tissue as an inert storage depot for lipids, and highlighted its role as an active endocrine organ that monitors and alters whole-body metabolism and maintains energy homeostasis. Since its identification in the mid-90's [20], the adipokine adiponectin (also known as Acrp30, AdipoQ and GBP28) has become best known as a regulator of insulin sensitivity. The two adiponectin receptor isoforms, AdipoR1 and AdipoR2, previously have been shown to be associated with increases in activities of AMP-activated protein kinase (AMPK) and peroxisome-proliferator activated receptor (PPARα). Recently, our group has shown that adiponectin is capable of inducing ceramidase activity through its receptors, which results in the hydrolysis of ceramide to form sphingosine and free fatty acid. Sphingosine, produced in this reaction, can go on to be phosphorylated by sphingosine kinase to produce sphingosine 1-phosphate (S1P), which functions as an important signaling molecule in a number of different cellular processes. The ceramide lowering effect of the adiponectin receptors only marginally depends on the activity of AMP kinase (AMPK), but AMPK can be activated through increasing the local S1P pool. Thus, this process appears to be a proximal event in adiponectin signaling, since it is a necessary step in adiponectin's induction of AMPK activation. These data support a previous model based on data from a heterologous system that connected the family of Progesterone and AdipoQ receptors (PAQRs), which includes AdipoR1 and AdipoR2, with ceramidase activity [10,28] and suggested a revised view of adiponectin signaling with sphingolipid metabolism at its core. Sphingolipids, such as ceramides and glucosylceramides, are an important class of bioactive lipids. The levels of these lipids change as

[1]Touchstone Diabetes Center, Department of Internal Medicine, The University of Texas Southwestern Medical Center, Dallas, TX 75390-8549, USA [2]Center for Metabolic and Degenerative Diseases, Institute of Molecular Medicine, University of Texas Health Science Center at Houston, Houston, TX 77030, USA [3]Department of Cell Biology, The University of Texas Southwestern Medical Center, Dallas, TX 75390-8549, USA

[4] William L. Holland and Jonathan Y. Xia contributed equally to this work.

*Corresponding author. Touchstone Diabetes Center, Department of Internal Medicine, University of Texas Southwestern Medical Center, 5323 Harry Hines Blvd., Dallas, TX 75390-8549, USA. Fax: +214 648 8720. E-mail: William.Holland@utsouthwestern.edu (W.L. Holland).

Received December 6, 2016 • Revision received December 27, 2016 • Accepted January 5, 2017 • Available online 12 January 2017

http://dx.doi.org/10.1016/j.molmet.2017.01.002

 © 2017 Published by Elsevier GmbH. This is an open access article under the CC BY-NC-ND license (http://creativecommons.org/licenses/by-nc-nd/4.0/).

a function of adipose tissue mass and functionality, and are partially driven by cellular availability of palmitoyl-CoA. Aberrant accumulation of ceramide, glucosylceramide, and GM3 ganglioside has been implicated in a multitude of metabolic processes, including atherosclerosis, insulin resistance, lipotoxic heart failure, β-cell apoptosis, and β-cell dysfunction (reviewed in [7]). In stark opposition, the phosphorylated sphingoid base Sphingosine 1-phosphate (S1P) is a potent inducer of proliferation and inhibitor of apoptosis [24]. The conversion of ceramide to S1P consists of deacylation of ceramide by ceramidase enzymes and a subsequent phosphorylation of sphingosine by one of two sphingosine kinase isoforms [21]. The opposing nature and simple 2-step conversion-process separating these lipids has led to speculation that the dynamic ratio of ceramide:S1P may constitute a physiological rheostat regulating in numerous cellular processes [24].

To gain further insights into the local physiological consequences of adiponectin and AdipoR-induced ceramidase activation we have embarked on two parallel approaches. Using a novel doxycycline-inducible model to allow for tissue-specific overexpression of acid ceramidase, we have determined that ceramidase activation in adipose or liver is sufficient to prevent or reverse diet-induced steatosis, insulin resistance, and glucose intolerance [29]. Here we have generated similar models allowing for AdipoR1 or AdipoR2 to be expressed under the control of a tetracycline response element (TRE-AdipoR1 or TRE-AdipoR2). We use these in order to determine which adiponectin receptor may have the most beneficial effects on glucose tolerance and whole body insulin sensitivity, and to compare and contrast adiponectin receptor action with a lysosomal ceramidase that does not promote S1P accumulation. Furthermore, we determine whether targeting of adiponectin receptors within hepatocytes or adipocytes provides the greatest metabolic improvements and evaluate the effects of adiponectin receptor agonists for their ability to faithfully recapitulate these effects and further enhance them in transgenic mice.

2. MATERIALS AND METHODS

2.1. Animals

All animal experimental protocols were approved by the Institutional Animal Care and Use Committee of University of Texas Southwestern Medical Center at Dallas. TRE-AdipoR1 or TRE-AdipoR2 mice were generated by subcloning the murine adiponectin receptor gene into a plasmid containing the TetO element. Following linearization, the construct was injected into C57/Bl6-derived blastocysts. Transgene-positive offspring were genotyped using PCR with the following primer sets: TRE-AdipoR1 forward, 5′-ACGTCCTGGTGGTGGGAGCAG and TRE-AdipoR1 reverse, 5′-TCATGAGGGTCCATGGTGATAC; TRE-AdipoR2 forward 5′-TGTGACATCTGGTTTCACTCTC and TRE-AdipoR2 reverse, 5′-TGGTGATACAAGGGACATCTTC.

The *Rosa26-loxP-stop-loxP-rtTA* and *Albumin-Cre* mice were lines were obtained from Jackson Laboratories. *Albumin-Cre* mice were bred with the *Rosa26-loxP-stop-loxP-rtTA* mice to achieve liver-specific expression of rtTA. This mouse was subsequently crossed to the TRE-R1 or TRE-R2 transgenic mice. The resulting triple transgenic mice expressed adiponectin receptor in liver only after exposure to doxycycline (Dox). All overexpression experiments were performed in a pure C57/Bl6 background. All experiments were conducted using littermate-controlled male mice. All Dox-chow diet (200 mg/kg Dox) or HFD-Dox (200 mg/kg Dox) experiments were initiated at approximately 6–12 weeks of age. To generate adipose-specific transgenic mice, the TRE-R1 or TRE-R2 mice were crossed with previously established Adiponectin-rtTA transgenic lines [23]. Wildtype mice for each experiment were rtTA-free or TRE-free littermates, which allowed for direct comparison between receptor transgenic and wt. For AdipoRon studies, mice were injected IP with 5 mg/kg of AdipoRon (Cayman) as previously described [17]. Serum glucose was monitored for 2 h post-injection.

2.2. Neutral ceramidase activity assay

Neutral ceramidase activity was determined by using NBD C12 ceramide as we have previously described [6].

2.3. Systemic tests

Glucose (2.5 g/kg, oral), insulin (0.75 U/kg, IP) and triglyceride (15 uL/g 20% intralipid, oral) were administered for tolerance tests as we previously described [29]. Hyperinsulinemic-euglycemic clamps were performed on conscious, unrestrained male C57 black WT and Alb-AC mice, as previously described [6,11].

2.4. Quantitative real-time PCR

Tissues were excised from mice and snap-frozen in liquid nitrogen. Total RNA was isolated following tissue homogenization in Trizol (Invitrogen, Carlsbad, CA) using a TissueLyser (MagNA Lyser, Roche) then isolated using an RNeasy RNA extraction kit (Qiagen). The quality and quantity of the RNA was determined by absorbance at 260/280 nm. cDNA was prepared by reverse transcribing 1 ug of RNA with an iScript cDNA Synthesis Kit (BioRad). Results were calculated using the threshold cycle method [14], with β-actin used for normalization.

2.5. Histology, immunohistochemistry (IHC)

The relevant adipose and liver tissues were excised and fixed in 10% PBS-buffered formalin for 24 h. Following paraffin embedding and sectioning (5 μm), tissues were stained with H&E.

2.6. Immunoblotting

Frozen tissue was homogenized in TNET buffer (50 mM Tris–HCl, pH 7.6, 150 mM NaCl, 5 mM EDTA, phosphatase inhibitors (Sigma–Aldrich) and protease inhibitors (Roche) and then centrifuged to remove any adipose layer present. After the addition of Triton X-100 (final concentration of 1%), protein concentrations were determined using a bicinchoninic acid assay (BCA) kit (Pierce). Proteins were resolved on 4–20% TGX gel (Bio-Rad) then transferred to nitrocellulose membranes (Protran). pAkt (Ser473, 4060) and total Akt (2920) (Cell Signaling Technology, Inc.) were used (1:1,000) for insulin signaling studies. Primary antibodies were detected using secondary IgG labeled with infrared dyes emitting at 700 nm (926-32220) or 800 nm (926-32211) (both at 1:5,000 dilutions) (Li-Cor Bioscience) and then visualized on a Li-Cor Odyssey infrared scanner (Li-Cor Bioscience). The scanned data were analyzed and quantitated using Odyssey Version 2.1 software (Li-Cor Bioscience).

2.7. Lipid quantifications

Sphingolipids were quantified as described previously by LC/ESI/MS/MS using a Shimadzu Nexera X2 UHPLC system coupled to a Shimadzu LCMS-8050 triple quadrupole mass spectrometer [6]. Lipid species were identified based on their molecular mass and fragmentation patterns, and verified by lipid standards. Diacylglycerol was quantified by direct-infusion mass spectrometry using an AB Sciex 5600+, as previously described [29].

2.8. AdipoRon treatment

Mice were injected IP with 5 mg/kg of AdipoRon (Cayman) as previously described [17]. Serum glucose was monitored for 2 h post-injection.

 © 2017 Published by Elsevier GmbH. This is an open access article under the CC BY-NC-ND license (http://creativecommons.org/licenses/by-nc-nd/4.0/).

2.9. Statistics

All results are provided as means ± s.e.m. All statistical analyses were performed using GraphPad Prism. Differences between the two groups over time (indicated in the relevant figure legends) were determined by a two-way analysis of variance for repeated measures. For comparisons between two independent groups, a Student's *t* test was used. Significance was accepted at $P < 0.05$.

3. RESULTS

We recently reported that FGF21 rapidly promotes adiponectin secretion and lowers hepatic ceramides. Curiously, FGF21 promoted an increase in accumulation of ceramides (Supplemental Figure 1A) and glucosylceramides (Supplemental Figure 1B) within the adipose tissue. As opposed to an increase in ceramidase activity in the liver (Supplemental Figure 1C, top), ceramidase activity in the adipose tissue was decreased by FGF21 (Supplemental Figure 1C, bottom). As this coincides with a decrease in adiponectin retained within the adipocyte, these data (and others) prompted us to consider if adiponectin receptors promote ceramidase activity within adipocytes to convey adiponectin actions within adipose tissue.

3.1. Overexpression of adiponectin receptors-1 or -2 in the adipose tissue reduces both adipose and hepatic ceramide levels and improves whole-body glucose and lipid homeostasis

Following a cross to our established Adiponectin-rtTA (ART) tetracycline transactivator mouse (Supplemental Figure 1D), founder lines (R1-Art or R2-Art) for TRE-AdipoR1 and TRE-AdipoR2 were screened for inducible-expression in response to a doxycycline-supplemented diet (200 mg/kg). For TRE-AdipoR2, founder lines were identified which allowed for an 8.6 fold increase in AdipoR2 mRNA levels, which required the presence of doxycycline and an ART allele (Supplemental Figure 1E). Following 10 days of doxycycline chow, ceramidase activity was increased in mesenteric and gonadal fat pads of Art-R1 and Art-R2 mice, without altering ceramidase activity in liver (Figure 1A). Under these conditions, the concentration of each major chain length of ceramide was diminished in mesenteric fat by AdipoR2 overexpression (Supplemental Figure 1F).

To evaluate the potential for adiponectin receptors to maintain glucose homeostasis via local signaling within the adipose tissue, we challenged Art-R1 and Art-R2 mice with 8 weeks of high fat diet (HFD) and 10 additional days of high fat diet supplemented with doxycycline (200 mg/kg) (HFD-dox). Prior to doxycycline, Art-R2 mice and wildtype mice displayed identical degrees of diet-induced glucose intolerance (Supplemental Figure 1G). However, after 10 days of doxycycline, Art-R2 mice had markedly improved glucose tolerance during an oral glucose tolerance test (OGTT) compared to wildtype littermates (Figure 1B). Lower serum insulin levels were measured for Art-R2 mice during fasting and glucose tolerance tests, which suggests improved insulin sensitivity (Supplemental Figure 1H). The rate of glucose disappearance in Art-R2 was not significantly different from wildtype mice (Supplemental Figure 1I), suggesting minimal effects on muscle insulin sensitivity. However, HFD-dox-fed Art-R1 (Figure 1C) and Art-R2 (Figure 1D) mice had substantially decreased blood glucose levels after insulin injection during an insulin tolerance test (ITT), suggesting enhanced insulin sensitivity in several other tissues. In order to unambiguously assess insulin sensitivity in Art-R1 and Art-R2 mice, we performed hyperinsulinemic-euglycemic clamp studies in cohorts of Art-R1, Art-R2, and WT littermate animals. The glucose infusion rate needed to maintain euglycemic conditions (149.9 ± 3.34 mg/dL R1wt vs 144.72 ± 3.01 mg/dL for Art-R1; 149.8 ± 3.13 mg/dL for R2wt versus 138.8 ± 5.78 mg/dL for Art-R2) was increased in both Art-R1 and Art-R2 mice compared to their littermate controls (Figure 1E, left panel), demonstrating that whole-body insulin sensitivity is improved. Whole body glucose disposal was not altered, suggesting minimal effects on muscle insulin action. At the same time, hepatic glucose production under hyperinsulinemic clamp conditions was suppressed more efficiently in Art-R2 mice compared to WT littermates (Figure 1E, right panel). These data suggest that adipocyte-specific overexpression of AdipoR2 attenuates diet-induced systemic insulin resistance by improving insulin sensitivity in the liver. Improvements in insulin sensitivity could not be explained by body weight (34.44 ± 2.48 g R1-wt versus 34.14 ± 5.94 g Art-R1; 39.72 ± 1.57 g for R2-wt versus 37.82 ± 2.56 g for Art-R2), glucose, or insulin levels achieved in the clamped state. The longer duration of dietary administration in Art-R2 experiments (15 weeks) prevents reasonable comparison to Art-R1 clamps performed 8 weeks after initiating high fat diet.

Adiponectin knockout mice appear to have aberrant lipolysis [18], which is particularly evident in the relative absence of insulin [36,37]. When orally challenged with triglyceride, Art-R1 and Art-R2 mice show improved clearance of lipid from the bloodstream; baseline circulating triglycerides were significantly lower in Art-R1 transgenic mice ($p < 0.05$) and trended lower in Art-R2 transgenic mice ($p = 0.057$) as compared to wildtype mice (Figure 1F). Moreover, hepatic triglyceride accumulation is also diminished in Art-R1 and Art-R2 mice (Figure 1G). Overexpression of AdipoR1/R2 in adipose tissue results in significantly lowered levels of ceramide species in the mesenteric (mWAT) and subcutaneous (sWAT) adipose depots following HFD-dox treatment. In Art-R1 mice, C18:0 ceramide levels were significantly reduced in both the mWAT and sWAT. As for the Art-R2 mice, C16:0, C18:0, and C:20:0 species were significantly lowered in mWAT and sWAT (Figure 1H). Glucosylceramides levels were also significantly lowered in adipose tissue of Art-R2 mice (Supplemental Figure 1J). This may suggest that AdipoR1 and AdipoR2 recruit ceramidases with different chain length specificities. Since acid ceramidase overexpression in adipose tissue prompts decreased circulating and hepatic ceramides [29], we addressed whether AdipoR1/2 related ceramidase activation could also diminish ceramides in serum and liver. Indeed, Art-R1 and Art-R2 mice have lower circulating ceramides for the majority of all major ceramide species, especially C16:0 ceramides (Figure 1I). The transgenic mice also displayed significantly ($p < 0.05$) lower C16 and C18 ceramides in the liver (Figure 1J).

3.2. Overexpression of adiponectin receptor-1 and -2 in the liver reduces hepatic ceramide levels and improves total body glucose and lipid homeostasis

We and others have previously shown that the adiponectin receptors AdipoR1 and AdipoR2 mediate the anti-diabetic metabolic actions of adiponectin. To investigate the liver-specific actions of adiponectin we generated an inducible, liver-specific AdipoR1 (Alb-R1) and AdipoR2 (Alb-R2) mouse, which combines three transgenic lines: the albumin promoter-driven Cre line, a transgenic line carrying a Rosa26 promoter-driven loxP-stop-loxP-reverse tetracycline-controlled transactivator (rtTA) gene (Rosa26-loxP-stop-loxP-rtTA), and a Tet-responsive AdipoR1 (TRE-R1) or AdipoR2 (TRE-R2) (Supplemental Figure 2A). Upon doxycycline induction, we found that ceramidase activity in liver lysates of Alb-R2 mice to be ~2 times that of WT (Supplemental Figure 2B).

To test whether the increased adiponectin receptor activity has a functional impact on ceramide levels in hepatocytes, we challenged the WT and Alb-R1 and -R2 mice with a high fat diet (60% calories

 © 2017 Published by Elsevier GmbH. This is an open access article under the CC BY-NC-ND license (http://creativecommons.org/licenses/by-nc-nd/4.0/).

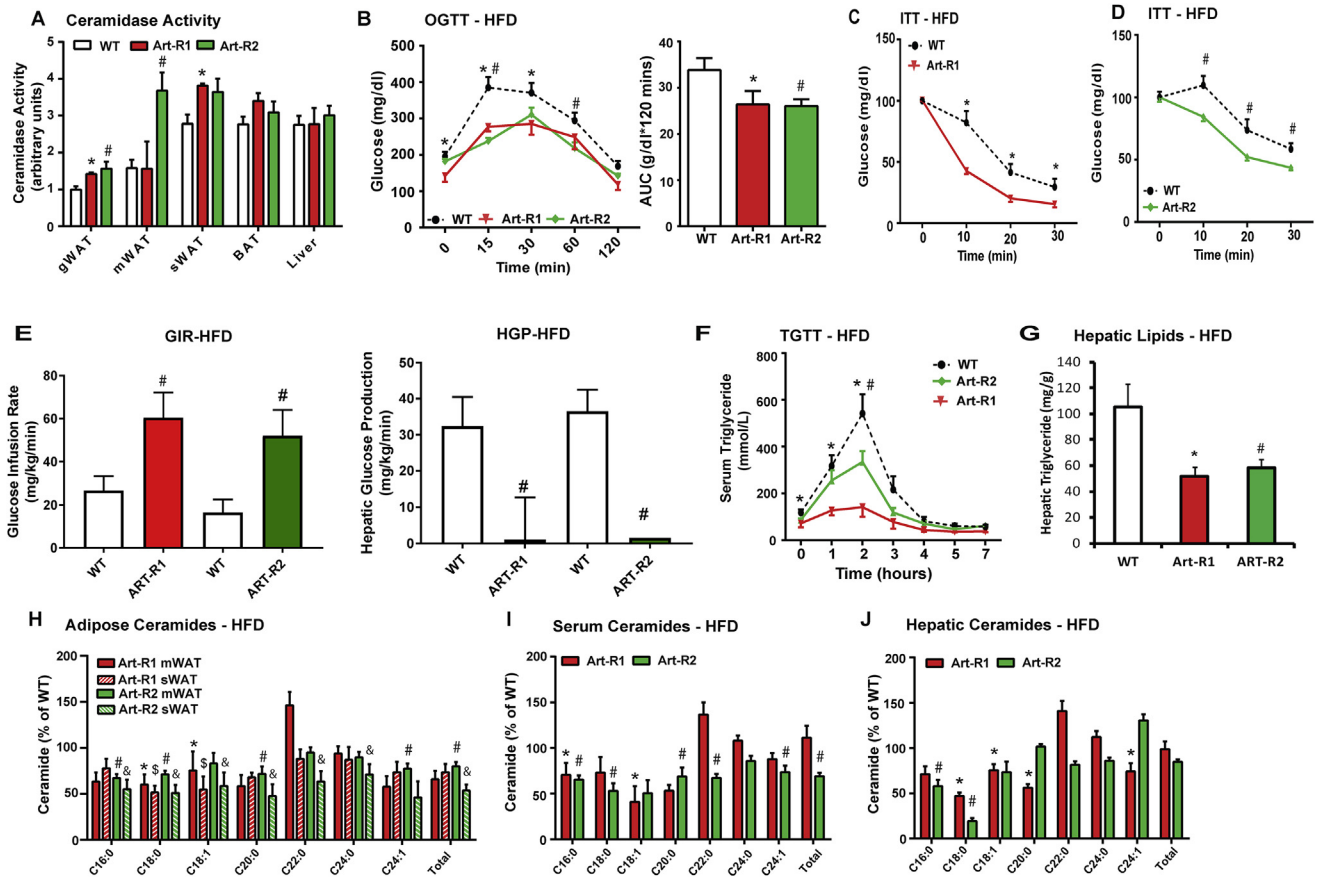

Figure 1: Inducible adipose-specific overexpression of AdipoR1/2 results in systemic improvements in glucose and lipid homeostasis. A) Analysis of neutral ceramidase activity from adipose depots and liver of Art-R1, Art-R2 mice, and WT littermates after 10 days of dox-Chow. **B)** After 8 weeks of HFD, mice were switched to HFD-dox. Circulating glucose levels were measured during an oral glucose tolerance test (OGTT, 2.5 g/kg glucose per oral gavage) 7 days after dox. **C)** Serum glucose levels during an ITT (0.75 U/kg, IP) of Art-R1 mice and WT littermates. **D)** Circulating glucose levels measured during an ITT (0.75 U/kg, IP) of Art-R2 mice and WT littermates. **E)** Glucose infusion rates (left) and hepatic glucose output (right) during hyperinsulinemic-euglycemic clamp experiments performed on conscious unrestrained 20-week-old WT and Art-R2 males or 15-week-old WT and Art-R1 males **F)** Circulating triglyceride (TG) levels were measured during an oral TG clearance test (20% intralipid, 15 uL/g body weight; single gavage) in Art-R1, Art-R2, and WT littermate controls. **G)** Hepatic TG content was enzymatically quantified. **H-J)** Ceramide species of the indicated chain lengths were quantified in mesenteric and inguinal adipose depots (H), serum (I) and liver (J) expressed as % of WT. All samples are from Art-R1, Art-R2 mice, and WT littermates after 8 weeks of HFD-dox challenge ($n = 6–8$/group), unless specified otherwise. * corresponds Art-R1 compared to WT littermates and # corresponds to Art-R2 compared to WT littermates. For Figure **I**, * corresponds to Art-R1 mWAT compared to WT mWAT, # corresponds to Art-R2 mWAT compared to WT mWAT, and & corresponds to Art-R2 sWAT compared to WT sWAT. *, #, &: $P < 0.05$.

from fat) containing 200 mg/kg doxycycline (HFD-dox). After 8 weeks of HFD-dox exposure, wildtype mice showed a 2.4 fold increase in hepatic ceramides compared to chow-fed controls (Supplemental Figure 2C). Both Alb-R1 and R2 mice showed a significant reduction in $C_{16:0}$ *hepatic* ceramide species (Figure 2A). In parallel, a significant lowering of $C_{16:0}$ and $C_{18:0}$ ceramide species was also observed in the *serum* (data not shown). Interestingly, AdipoR2 overexpression, but not AdipoR1, also resulted in an increase in hepatic sphingosine-1-phosphate (Figure 2A). Our recent work has shown that alterations in hepatic ceramides levels can result in changes in adipose tissue ceramide levels. Hepatic overexpression of AdipoR2 resulted in a corresponding lowering of adipose levels of lactosyl, glucosyl, and total ceramide species (Figure 2B). Liver overexpression of AdipoR1 resulted in a corresponding lowering of adipose lactosyl and glucosyl ceramide species (Figure 2B).

To determine the role of hepatic overexpression of AdipoR1 and R2 in diet-induced obesity and associated metabolic disorders, we exposed Alb-R1, Alb-R2, and WT littermate control mice to HFD-dox for 10 weeks. Body weights of the mice were monitored on a weekly basis during the HFD feeding period. We observed similar weight gain curves for the Alb-R1, Alb-R2, and WT mice and comparable body weights at the end of the 10 weeks of HFD-dox exposure (Supplemental Figure 2E). However, compared to WT controls, Alb-R1 mice exhibited reduced blood glucose levels during the oral glucose tolerance test (OGTT) (Figure 2C), indicating an improvement in systemic glucose tolerance. Additionally, the plasma insulin levels during the OGTT were also lower in the Alb-R1 mice (Figure 2D). Similarly, Alb-R2 mice also exhibited marked lowering of serum glucose levels during the OGTT, while also exhibiting lowered plasma insulin levels compared to WT controls (Figure 2E and F). Both Alb-R1 and Alb-R2 transgenics required a higher glucose infusion rate to achieve a euglycemia of 120 mg/dL during the hyperinsulinemic-euglycemic clamp compared to their WT littermates, thus, confirming their overall improvement in whole-body insulin sensitivity (Figure 2G, left panel). Alb-R2 mice and their wildtype littermates were older than Alb-R1 mice at the time of clamp, which likely explains the more severe insulin resistance. Whole body glucose disposal was not altered (Supplemental Figure 2E), suggesting minimal effects on muscle insulin action. Hepatic glucose production under hyperinsulinemic clamp conditions was suppressed more efficiently in Alb-R1 and Alb-R2 mice compared to WT littermates

 © 2017 Published by Elsevier GmbH. This is an open access article under the CC BY-NC-ND license (http://creativecommons.org/licenses/by-nc-nd/4.0/).

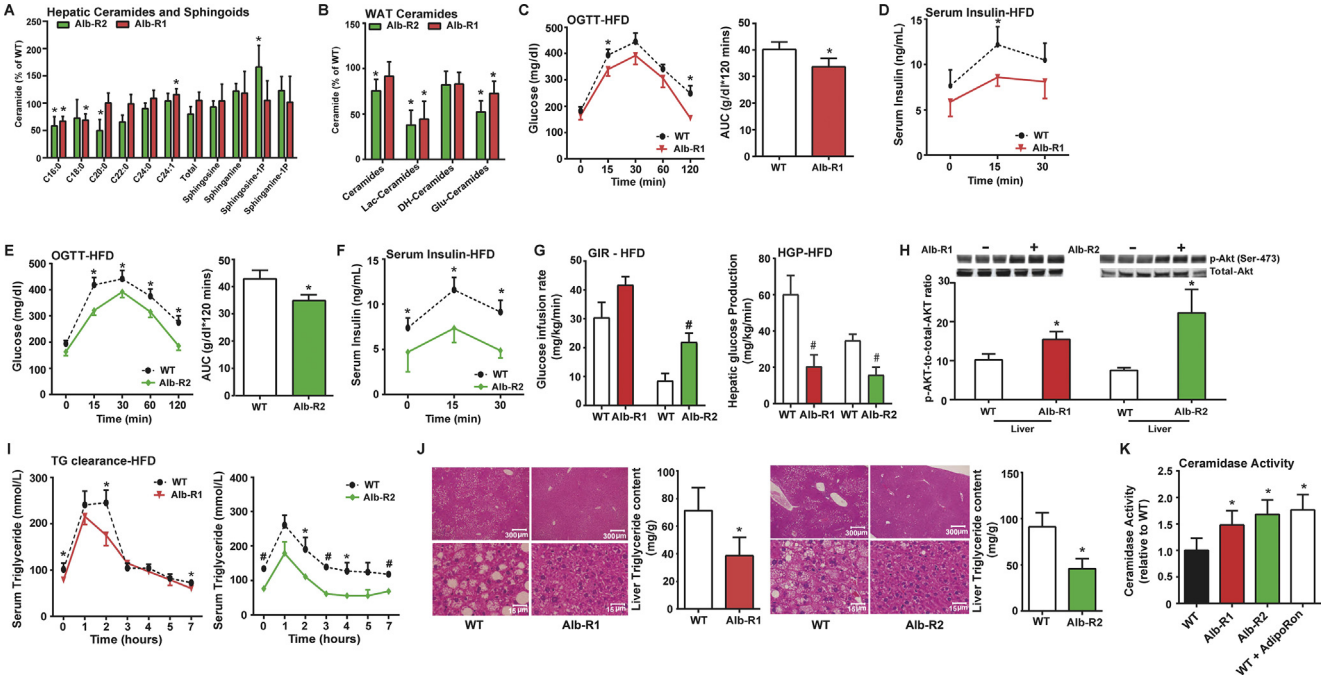

Figure 2: Inducible liver-specific overexpression of either AdipoR1 or AdipoR2 results in significantly reduced $C_{16:0}$ ceramide species in the liver and improved total body glucose homeostasis and reduced hepatic lipid accumulation under HFD feeding. A) Analysis of liver ceramide and sphingoid species from Alb-R1 and Alb-R2 mice and WT littermates. **B)** Total WAT ceramide and sphingoid species in Alb-R1 and Alb-R2 mice and WT littermates. **C)** Circulating glucose levels were measured during an oral glucose tolerance test (OGTT) for Alb-R1 mice (2.5 g/kg glucose per oral gavage). **D)** Serum insulin levels during the OGTT were quantified via ELISA for Alb-R1 mice. **E)** Circulating glucose levels were measured during an oral glucose tolerance test (OGTT) for Alb-R2 mice (2.5 g/kg glucose per oral gavage). **F)** Serum insulin levels during the OGTT were quantified via ELISA for Alb-R2 mice. **G)** Glucose infusion rates (left) and hepatic glucose output (right) during hyperinsulinemic-euglycemic clamp experiments performed on conscious unrestrained 20-week-old WT and Alb-R2 males and 15 week old WT and Alb-R1 males. **H)** Representative immunoblots of phosphorylated and total Akt of insulin stimulated Alb-R1, Alb-R2, and control mice, shown in triplicate. **I)** Circulating triglyceride (TG) levels were measured during an oral TG clearance test (20% intralipid, 15 uL/g body weight; single gavage) in Alb-R1 (left), Alb-R2 (right) mice and WT littermate controls. **J)** Representative H&E stained images of WT and Alb-R1 livers (left) and Alb-R2 livers (right). Bar graphs represent quantification of liver triglyceride levels. **K)** Analysis of neutral ceramidase activity from liver of WT, Alb-R1, Alb-R2 mice post dox treatment and WT mice treated with AdipoRon. All samples are from Alb-R1, Alb-R2 mice, and WT littermates after 10 weeks of HFD −dox challenge (n = 6), unless specified otherwise. $^*P < 0.05$, #P < 0.01 by Student's *t* test.

(Figure 2G, right panel). Furthermore, insulin signaling in the liver of Alb-R1 and Alb-R2 mice was assessed by insulin-stimulated phosphorylation of Akt. After an injection of insulin, p-Akt levels were greatly increased in the liver of Alb-R1 and Alb-R2 transgenic animals, reflecting improved insulin sensitivity as compared to wildtype mice (Figure 2H). PPARα target genes were assessed to determine the potential contributions of this transcription factor (Supplemental Figure 2F); AdipoR2, but not AdipoR1 increased expression of PPARα and Acox1.

In order to assess the effects of liver overexpression of AdipoR1 and R2 on *systemic* lipid homeostasis, we performed oral triglyceride tolerance tests in Alb-R1, Alb-R2 and WT mice. Both Alb-R1 and Alb-R2 had significantly lowered basal serum triglyceride levels compared to WT and at the same time exhibited higher excursion of triglyceride in serum compared to their WT littermate controls (Figure 2I). Furthermore, the enhanced triglyceride clearance is more pronounced in Alb-R2 mice compared to Alb-R1 mice. Prolonged HFD exposure often causes the accumulation of lipids in the liver. Considering that serum adiponectin levels are inversely correlated with hepatic triglyceride content [26], we expected both the Alb-R1 and Alb-R2 mouse livers to have less lipid accumulation compared to WT controls. Livers were harvested from Alb-R1 and Alb-R2 mice after 10 weeks of HFD-dox diet. Histologically, both Alb-R1 (left) and R2 (right) livers exhibited substantially less lipid accumulation compared to WT controls (Figure 2J). Biochemical analysis of hepatic triglyceride content of Alb-R1 and Alb-R2 livers showed that both Alb-R1 and Alb-R2 exhibited almost a 50% decrease in hepatic triglyceride accumulation compared to WT mice (Figure 2J). Under these conditions of diet-induced obesity, we found that Alb-R1 and Alb-R2 mice both showed significantly greater neutral ceramidase activity in the liver as compared to WT controls (Figure 2K). Moreover, following injection of the adiponectin receptor agonist AdipoRon, livers from wt mice showed a 76% increase in ceramidase activity from liver lysates. These data suggest that adiponectin receptor agonism may be a beneficial therapeutic for the treatment of hyperglycemia and function via a ceramide-lowering mechanism.

3.3. The metabolic improvements of adiponectin receptor overexpression in the liver are adiponectin dependent

The liver is the main target tissue of adiponectin [3], and AdipoR2 is the dominant adiponectin receptor isoform in the liver [32]. To determine whether the beneficial effects of adiponectin receptor overexpression is ligand dependent, we crossed the Alb-R1 and Alb-R2 mice with the adiponectin knockout mice (APN KO) previously generated in our lab [16] to generate a mouse devoid of endogenous adiponectin but still overexpressing AdipoR1 (R1-KO) or 2 (R2-KO) in the liver. This allows an advantage over cultured-cell systems, which rely heavily and adiponectin-containing serum for growth factors.

To test whether increasing adiponectin receptor activity alone has a functional impact on hepatic ceramide levels in the absence of

 © 2017 Published by Elsevier GmbH. This is an open access article under the CC BY-NC-ND license (http://creativecommons.org/licenses/by-nc-nd/4.0/).

adiponectin, we challenged R1-KO and R2-KO mice and APN KO mice with 10 weeks of HFD-dox and quantified hepatic ceramides in both groups. We found that there were no significant differences in hepatic ceramide species between R1-KO, R2-KO, and their APN KO littermate controls (Figure 3A). We observed that there were no significant differences in weight gain between the APN KO and R2-KO during the 10 week period of HFD-dox feeding, and both groups had comparable body weights at the end of the 10 weeks of HFD-dox feeding (Supplemental Figure 3A). Metabolically, both groups developed insulin resistance and hyperglycemia as a result of the HFD-dox feeding. R1-KO and R2-KO mice did not exhibit any improvements in glucose homeostasis during the OGTT at the end of the HFD-dox challenge compared to the APN KO mice (Figure 3B,C). Additionally, R2-KO mice had higher, but insignificant, levels of plasma insulin during the OGTT compared to its APN KO counterpart (Supplemental Figure 3B). Insulin signaling in the liver of R2-KO and APN KO mice was assessed by insulin-stimulated phosphorylation of Akt. After 15 min of insulin stimulation, p-Akt levels in R2-KO mouse livers are similar to the levels in APN KO, thus indicating that insulin signaling was not improved (Supplemental Figure 3C). Overall, in the absence of adiponectin, liver specific overexpression of AdipoR2 loses its beneficial effects on glucose homeostasis and insulin sensitivity that was previously observed on an adiponectin-wildtype background.

In order to assess whether there were improvements in systemic lipid homeostasis in the R1-KO and R2-KO mice, we performed a triglyceride clearance test by orally gavaging lipid to R1-KO, R2-KO and APN KO mice. Although R2-KO peaked at lower levels than APN KO the overall rate of triglyceride clearance between R2-KO and APN KO was not increased (Figure 3D). No changes in serum triglyceride clearance were observed between R1-KO mice and APN KO littermate controls (Figure 3E). Livers harvested from the R2-KO and APN KO mice after 10 weeks of HFD-dox were not different histologically (Supplemental Figure 3D). Livers from both groups had hepatic steatosis as a result of the HFD challenge, and biochemical analysis of hepatic triglyceride content of R2-KO and APN-KO livers showed that both groups had similar levels of hepatic triglyceride accumulation. Therefore, in the absence of its ligand adiponectin, liver overexpression of AdipoR1 or AdipoR2 fails to improve total body lipid homeostasis and reduce hepatic triglyceride content.

Past work done by Okada-Iwabu and colleagues has shown that a small molecule that binds to and activates adiponectin receptors (AdipoRon) could ameliorate insulin resistance and glucose intolerance in mice fed a high fat diet [17] by similar cellular mechanisms as adiponectin. Thus, we tested whether providing AdipoRon to APN R1-KO, R2-KO, and APN KO mice would elicit a similar effect on their glucose homeostasis. We fed R1-KO, R2-KO, and APN KO a HFD-dox for 10 weeks and at the end of the 10 weeks, AdipoRon was injected to assess effects on glucose and ceramide levels. Two hours after AdipoRon injection, we observed that R2-KO mice had a more robust lowering of serum glucose (73% of basal) compared to APN KO controls (92% of basal) (Figure 3F). No changes were observed in R1-KO mice and APN KO littermate controls post-injection (Figure 3G). Only in R2-KO mice did we observe notable changes in hepatic ceramide content following AdipoRon, as C16 and C18 ceramides were reduced by 25%. Thus, the metabolically-beneficial effect of liver AdipoR2 overexpression on systemic glucose homeostasis is restored upon stimulation by the ligand AdipoRon; however, these data do not rule out the possibility that AdipoRon also targets AdipoR1.

3.4. AdipoR2 overexpression in adipose tissue or liver is capable of rescuing diabetic phenotype in *ob/ob* mice

Past studies have shown that in insulin-resistant *ob/ob* mice, the expression levels of both AdipoR1 and AdipoR2 are significantly decreased in tissues [25]. In order to determine whether overexpression of adiponectin receptors in adipose tissue or liver is capable of ameliorating the insulin resistance and glucose intolerance exhibited

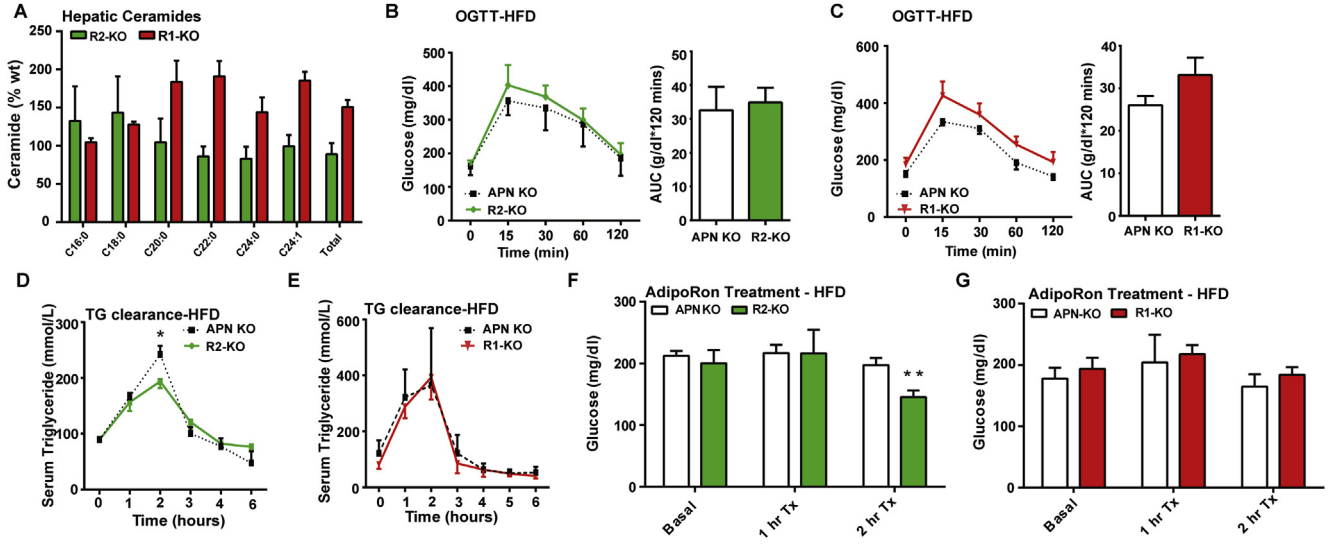

Figure 3: The metabolic improvements of adiponectin receptor overexpression in the liver are adiponectin dependent. A) Analysis of liver ceramide species from R2-KO mice and APN KO littermates. **B)** Circulating glucose levels were measured during an oral glucose tolerance test (OGTT) for R2-KO and APN KO mice (2.5 g/kg glucose per oral gavage). **C)** Circulating glucose levels were measured during an oral glucose tolerance test (OGTT) for R1-KO and APN KO mice (2.5 g/kg glucose per oral gavage). **D)** Circulating triglyceride (TG) levels were measured during an oral TG clearance test (20% intralipid, 15 uL/g body weight; single gavage) in R2-KO and APN KO littermate controls. **E)** Circulating triglyceride (TG) levels were measured during an oral TG clearance test (20% intralipid, 15 uL/g body weight; single gavage) in R1-KO and APN KO littermate controls. **F)** Serum glucose levels were measured before and after IP injection of AdipoRon (5 mg/kg) in APN KO and R2-KO mice after 10 weeks of HFD-dox challenge. **G)** Serum glucose levels were measured before and after IP injection of AdipoRon (5 mg/kg) in APN KO and R2-KO mice after 10 weeks of HFD-dox challenge. $^{*}P < 0.05$, $^{**}P < 0.01$ by Student's *t* test.

 © 2017 Published by Elsevier GmbH. This is an open access article under the CC BY-NC-ND license (http://creativecommons.org/licenses/by-nc-nd/4.0/).

in *ob/ob* mice, we crossed the Art-R2 and Alb-R2 transgenic models into the *ob/ob* genetic background. In addition, we also bred adipose or liver-specific overexpression of acid ceramidase (Art-AC and Alb-AC respectively) into *ob/ob* genetic background to study whether direct lowering of ceramides in those metabolic tissues can rescue the ob/ob phenotype. Adipose-specific overexpression of R2 and AC, *ob/ob*$^{Art\text{-}R2}$ and *ob/ob*$^{Art\text{-}AC}$ respectively, showed marked reductions in WAT ceramide levels after 10 days of induction with dox chow (Figure 4A). This was especially evident in mWAT where transgene expression was the highest. In addition, *ob/ob*$^{Art\text{-}R2}$ had a significant lowering of mWAT $C_{16:0}$ ceramide species whereas *ob/ob*$^{Art\text{-}AC}$ failed to exhibit a significant change in this chain length of ceramide. Moreover, deoxyceramide accumulation was reduced by AdipoR2 overexpression but not by AC overexpression (Supplemental Figure 4). The lowering of WAT deoxyceramide and $C_{16:0}$ ceramide in *ob/ob*$^{Art\text{-}R2}$ corresponded with improvements in glucose homeostasis during an OGTT compared to *ob/ob* mice. *ob/ob*$^{Art\text{-}AC}$ mice, however, did not exhibit any improvements in glucose homeostasis compared to *ob/ob* littermate controls (Figure 4B).

To test whether *liver* overexpression of AdipoR2 (*ob/ob*$^{Alb\text{-}R2}$) or acid ceramidase (*ob/ob*$^{Alb\text{-}AC}$) is capable of rescuing the *ob/ob* phenotype, we put *ob/ob*, *ob/ob*$^{Alb\text{-}R2}$, and *ob/ob*$^{Alb\text{-}AC}$ mice on chow-dox diet for 10 days and then assessed glucose homeostasis with an OGTT. We found that *ob/ob*$^{Alb\text{-}R2}$ mice have markedly lowered serum glucose levels during the OGTT compared to *ob/ob* control, indicating vast improvements in glucose clearance (Figure 4C). Although *ob/ob*$^{Alb\text{-}AC}$ exhibited significantly lowered basal serum glucose levels compared to *ob/ob* controls at some time points, the overall rate of glucose clearance in *ob/ob*$^{Alb\text{-}AC}$ was not changed compared to *ob/ob* mice (Figure 4C). In addition, *ob/ob*$^{Alb\text{-}R2}$ and *ob/ob*$^{Alb\text{-}AC}$ had similar levels of serum insulin, which were lower compared to *ob/ob* during OGTT (Figure 4D). We also wanted to assess the effect of AdipoRon on ceramide lowering in the absence of leptin action. Two hours after injection with AdipoRon, leptin-deficient *ob/ob* mice show a marked reduction in hepatic ceramide levels suggesting that the ceramide-lowering actions of adiponectin are intact with this small molecule receptor agonist (Figure 4E).

4. DISCUSSION

Here, we report the first mouse models demonstrating inducible overexpression of adiponectin receptors. Our inducible AdipoR models bypass the compensatory mechanisms and developmental issues present in constitutive models of adiponectin overexpression and give us the opportunity to study acute modifications of AdipoR induced metabolic improvements in adult mice. With this novel system, we demonstrate that the acute depletion of ceramide via adiponectin receptor expression and activation in hepatocytes or adipocytes of adult mice can decrease hepatic steatosis while simultaneously improving systemic glucose tolerance and insulin sensitivity in adult mice with diet-induced obesity. These studies highlight the important role for adiponectin action within the adipocyte and further support the concept of prominent cross-talk between the liver and adipose tissue that allows for equilibration of sphingolipids between the two tissues.

These studies link adiponectin-induced ceramidase activity to metabolic improvements of non-alcoholic fatty liver disease and systemic insulin resistance in rodents. Similar to our recent report of acid ceramidase overexpression we find that adiponectin receptors functionally prevent accumulation of C16 and C18 ceramides in DIO mice.

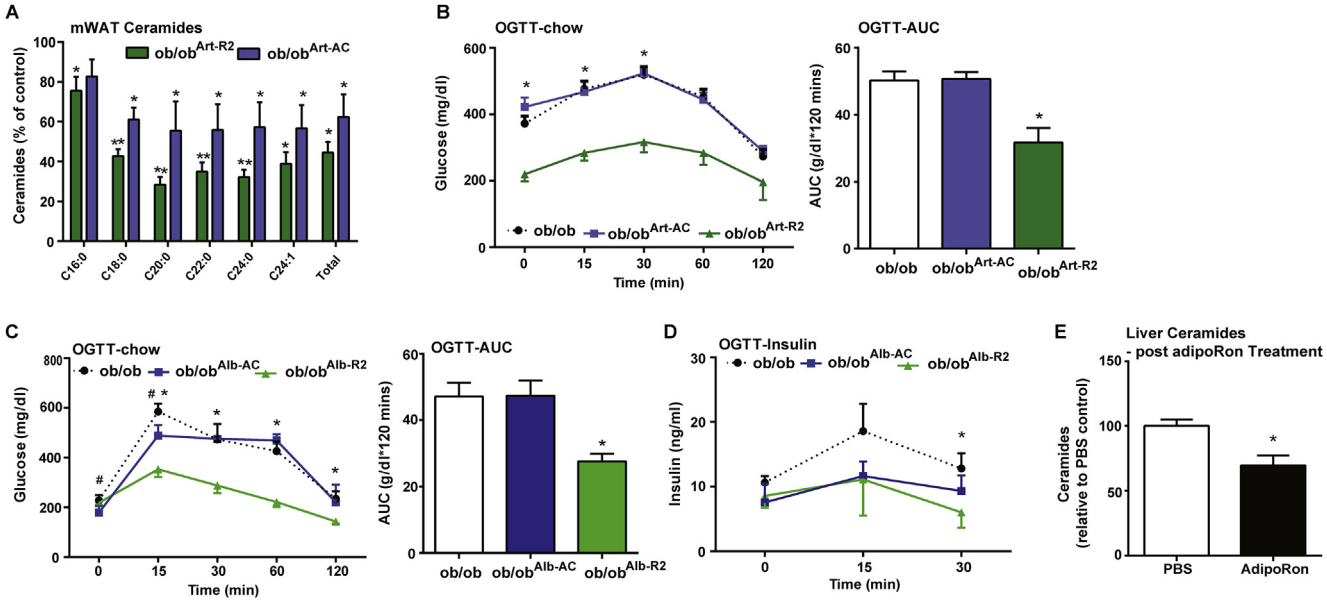

Figure 4: Overexpression of adiponectin receptors, but not acid ceramidase, rescues glucose homeostasis in ob/ob mice. A) Ceramide species of the indicated chain lengths were quantified in mesenteric and inguinal adipose depots from ob/ob mice following 2 weeks of dox-induced overexpression to drive Art-AdipoR2 or Art-Acid Ceramidase (AC). Data were quantified and expressed as % of wildtype ob/ob control. **B)** Circulating glucose levels were measured during an oral glucose tolerance test (OGTT) (2.5 g/kg glucose per oral gavage) in *ob/ob*, *ob/ob Art-AC*, and *ob/ob Art-AdipoR2* transgenic mice **C)** Circulating glucose levels were measured during an oral glucose tolerance test (OGTT) (2.5 g/kg glucose per oral gavage) after 10 days of dox-induced expression of AdipoR2 or Acid Ceramidase in the liver of *ob/ob* mice (* depicts *ob/ob* vs *ob/ob*$^{Alb\text{-}R2}$, $^{\#}$ depicts *ob/ob* vs *ob/ob*$^{Alb\text{-}AC}$). **D)** Insulin levels before and during the OGTT were measured by ELISA. **E)** Total ceramide levels were quantified in livers from *ob/ob* mice following 2 h of AdipoRon or PBS control treatment. $^{*,\#}P < 0.05$ by Student's *t* test.

 © 2017 Published by Elsevier GmbH. This is an open access article under the CC BY-NC-ND license (http://creativecommons.org/licenses/by-nc-nd/4.0/).

We found that $C_{16:0}$ and $C_{18:0}$ ceramide levels to be ~60% of WT in livers of Alb-R1 and AlbR2 mice, which are the ceramide subspecies that most prominently contribute to the development of NAFLD and hepatic insulin resistance. Consistent with our findings, recent work has shown that mice with ceramide synthase 6 deficiency ($cerS6^{\Delta/\Delta}$) exhibit reduced $C_{16:0}$ ceramide levels and are protected from high fat diet-induced obesity and glucose intolerance [27]. By contrast, heterozygous deletion of ceramide synthase 2 promotes a paradoxical increase in $C_{16:0}$ ceramides to confer greater susceptibility to diet induced insulin resistance [19].

Preclinical models indicate roles for adiponectin in the maintenance of hepatic lipid metabolism. Adiponectin overexpression prevents accumulation of triglycerides or the deleterious lipid metabolites diacylglycerols or ceramides [5,8]. Direct manipulation of adiponectin expression demonstrates a potential causal relationship between adiponectin signaling and steatosis [2]. Conversely, genetic ablation of adiponectin in leptin-deficient (*ob/ob*) mice further exacerbates hepatic triglyceride accumulation [4]. Hepatic steatosis is just an initial step in the progression of non-alcoholic steatohepatitis (NASH), and can ultimately enhance risk for cirrhosis and hepatocarcinoma. Adiponectin null mice develop fibrotic steatohepatitis and adenomas when maintained on high fat diets for 48 weeks [1] but not in response to shorter-term diet administration [13,35]. Administration of recombinant adiponectin in rodents results in beneficial effects on lipid metabolism, such as enhancing lipid clearance and increasing fatty acid oxidation in muscle and liver [30,33]. Delivery of adenoviral adiponectin can attenuate hepatomegaly, steatosis, and liver injury in mice with NASH [31]. Our studies suggest that adiponectins' anti-steatotic actions occur by local effects of ceramide-lowering in the liver, where targeted degradation of ceramides with acid ceramidase decreases hepatic lipid uptake and lipogenic gene expression [29]. Additionally, adiponectins' effects locally within the adipocyte contribute to enhanced lipid clearance mediated locally via AdipoR1 and AdipoR2, protecting non-adipocytes from excess lipid exposure.

Studies with genetic manipulation of adiponectin receptors show similar trends as adiponectin itself, and human single nucleotide polymorphisms in AdipoR1 or AdipoR2 are significantly associated with hepatic triglyceride accumulation [9,22] and enhanced risk for cirrhosis [15]. Adenoviral-mediated overexpression of either adiponectin receptor is sufficient to stimulate lipid oxidation and diminish hepatic triglyceride content [34]. By contrast, mice lacking both isoforms of the adiponectin receptors display elevated hepatic triglyceride accumulation. Our data suggest that activation of either isoform of adiponectin receptor will decrease hepatic steatosis and provide glycemic benefit. These studies provide strong preclinical evidence that adiponectin receptor agonism may be a powerful therapeutic tool. We show here for the first time that AdipoRon stimulates a ceramidase activity and can activate the adiponectin receptors to induce its metabolic beneficial effects when adiponectin is not present.

Importantly, the actions of adiponectin receptors critically rely on adiponectin for their functional lowering of ceramides and subsequent improvements in glucose and lipid homeostasis. This study adds strong *in vivo* genetic support that AdipoRs are indeed the cognate receptors that convey adiponectin actions. This challenges our previous notion that these receptors indeed have a strong basal activity and suggest that it is very difficult to eliminate adiponectin from culture systems where it is present in FBS-containing medium, which is enriched in bovine adiponectin.

Collectively, our data suggest that the lowering of ceramides is a critical player in adiponectin-induced improvements in non-alcoholic fatty liver disease and hepatic insulin resistance in mice with diet-induced obesity. Our data also demonstrate that the induction of AC activity is insufficient to rescue metabolic syndrome in *ob/ob* mice, while AdipoR2 overexpression is sufficient. Several key differences in these two approaches have been noted. First, adiponectin receptors lower more chain lengths of ceramides with diet induced obesity, suggesting that it is a potential novel therapeutic target. Additionally, AdipoR-induced ceramidase activity cleaves additional species like deoxyceramides, which may be more cytotoxic because of the limited pathways for metabolizing these alanine (rather than serine) derived sphingolipids. Unlike AC overexpression in the liver, AdipoR2 overexpression results in a significant increase in hepatic S1P levels. S1P has been shown in the past to induce AMPK, a major downstream effector of adiponectin [12]. Thus, a possible explanation of why AdipoR2 overexpression is capable of rescuing ob/ob phenotype is that it is an essential initiator of the broad spectrum of adiponectin action. Thus, orally active small-molecule adiponectin receptor agonists, such as AdipoRon, could potentially be an important therapeutic agent for patients with non-alcoholic fatty liver disease, diabetes, or other comorbidities of the metabolic syndrome [17].

AUTHOR CONTRIBUTIONS

WLH and JYX are co-first authors. WLH designed the studies, carried out the research, interpreted the results, wrote the manuscript and is responsible for the integrity of this work. JYX designed the studies, carried out the research, interpreted the results, and wrote portions of the manuscript. JAJ, KS, MJP, AXS, EQS, TST, and RG assisted in study design, performed research, and reviewed the manuscript. PES designed the study, analyzed the data and reviewed and revised the manuscript. All authors approved the final version of the manuscript.

ACKNOWLEDGEMENTS

We thank Dr. Bob Hammer and the Transgenic Core Facility at UTSW for the generation of the transgenic lines, John Shelton and the Histology Core for assistance with histology and the UTSW Metabolic Core Unit for help in phenotyping. We acknowledge support from the National Institutes of Health (grants R01-DK55758, R01-DK99110 and P01-DK88761 to PES). WLH is supported by a R00-DK094973 and JDRF Award 5-CDA-2014-185-A-N. JYX is supported by a NIH fellowship F30-DK100095. JAJ is supported by NIH fellowship F30-DK108534. MJP is supported by a fellowship from the NW NARCH and NIH T32-GM008203.

CONFLICT OF INTEREST

The authors declare no conflicts of interest.

APPENDIX A. SUPPLEMENTARY DATA

Supplementary data related to this article can be found at http://dx.doi.org/10.1016/j.molmet.2017.01.002.

REFERENCES

[1] Asano, T., Watanabe, K., Kubota, N., Gunji, T., Omata, M., Kadowaki, T., et al., 2009. Adiponectin knockout mice on high fat diet develop fibrosing steatohepatitis. Journal of Gastroenterology and Hepatology 24(10):1669–1676.

[2] Asterholm, I.W., Scherer, P.E., 2010. Enhanced metabolic flexibility associated with elevated adiponectin levels. American Journal of Pathology 176(3): 1364–1376.

 © 2017 Published by Elsevier GmbH. This is an open access article under the CC BY-NC-ND license (http://creativecommons.org/licenses/by-nc-nd/4.0/).

[3] Halberg, N., Schraw, T.D., Wang, Z.V., Kim, J.Y., Yi, J., Hamilton, M.P., et al., 2009. Systemic fate of the adipocyte-derived factor adiponectin. Diabetes 58(9):1961–1970.

[4] Holland, W.L., Adams, A.C., Brozinick, J.T., Bui, H.H., Miyauchi, Y., Kusminski, C.M., et al., 2013. An FGF21-adiponectin-ceramide Axis controls energy expenditure and insulin action in mice. Cell Metabolism 17(5): 790–797.

[5] Holland, W.L., Brozinick, J.T., Wang, L.P., Hawkins, E.D., Sargent, K.M., Liu, Y., et al., 2007. Inhibition of ceramide synthesis ameliorates glucocorticoid-, saturated-fat-, and obesity-induced insulin resistance. Cell Metabolism 5(3):167–179.

[6] Holland, W.L., Miller, R.A., Wang, Z.V., Sun, K., Barth, B.M., Bui, H.H., et al., 2011. Receptor-mediated activation of ceramidase activity initiates the pleiotropic actions of adiponectin. Nature Medicine 17(1):55–63.

[7] Holland, W.L., Summers, S.A., 2008. Sphingolipids, insulin resistance, and metabolic disease: new insights from in vivo manipulation of sphingolipid metabolism. Endocrine Reviews 29(4):381–402.

[8] Iwabu, M., Yamauchi, T., Okada-Iwabu, M., Sato, K., Nakagawa, T., Funata, M., et al., 2010. Adiponectin and AdipoR1 regulate PGC-1alpha and mitochondria by Ca(2+) and AMPK/SIRT1. Nature 464(7293):1313–1319.

[9] Kim, J.Y., van de Wall, E., Laplante, M., Azzara, A., Trujillo, M.E., Hofmann, S.M., et al., 2007. Obesity-associated improvements in metabolic profile through expansion of adipose tissue. The Journal of Clinical Investigation 117(9):2621–2637.

[10] Kotronen, A., Yki-Jarvinen, H., Aminoff, A., Bergholm, R., Pietilainen, K.H., Westerbacka, J., et al., 2009. Genetic variation in the ADIPOR2 gene is associated with liver fat content and its surrogate markers in three independent cohorts. European Journal of Endocrinology 160(4):593–602.

[11] Kupchak, B.R., Garitaonandia, I., Villa, N.Y., Smith, J.L., Lyons, T.J., 2009. Antagonism of human adiponectin receptors and their membrane progesterone receptor paralogs by TNFalpha and a ceramidase inhibitor. Biochemistry 48(24):5504–5506.

[12] Kusminski, C.M., Holland, W.L., Sun, K., Park, J., Spurgin, S.B., Lin, Y., et al., 2012. MitoNEET-driven alterations in adipocyte mitochondrial activity reveal a crucial adaptive process that preserves insulin sensitivity in obesity. Nature Medicine 18(10):1539–1549.

[13] Levine, Y.C., Li, G.K., Michel, T., 2007. Agonist-modulated regulation of AMP-activated protein kinase (AMPK) in endothelial cells. Evidence for an AMPK -> Rac1 -> Akt -> endothelial nitric-oxide synthase pathway. Journal of Biological Chemistry 282(28):20351–20364.

[14] Liu, Q., Yuan, B., Lo, K.A., Patterson, H.C., Sun, Y., Lodish, H.F., 2012. Adiponectin regulates expression of hepatic genes critical for glucose and lipid metabolism. Proceedings of the National Academy of Sciences of the United States of America 109(36):14568–14573.

[15] Livak, K.J., Schmittgen, T.D., 2001. Analysis of relative gene expression data using real-time quantitative PCR and the 2(-Delta Delta C(T)) method. Methods 25(4):402–408.

[16] Namvaran, F., Rahimi-Moghaddam, P., Azarpira, N., Nikeghbalian, S., 2012. The association between adiponectin (+45T/G) and adiponectin receptor-2 (+795G/A) single nucleotide polymorphisms with cirrhosis in Iranian population. Molecular Biology Reports 39(3):3219–3223.

[17] Nawrocki, A.R., Rajala, M.W., Tomas, E., Pajvani, U.B., Saha, A.K., Trumbauer, M.E., et al., 2006. Mice lacking adiponectin show decreased hepatic insulin sensitivity and reduced responsiveness to peroxisome proliferator-activated receptor gamma agonists. Journal of Biological Chemistry 281(5):2654–2660.

[18] Okada-Iwabu, M., Yamauchi, T., Iwabu, M., Honma, T., Hamagami, K., Matsuda, K., et al., 2013. A small-molecule AdipoR agonist for type 2 diabetes and short life in obesity. Nature 503(7477):493–499.

[19] Qiao, L., Kinney, B., Schaack, J., Shao, J., 2011. Adiponectin inhibits lipolysis in mouse adipocytes. Diabetes 60(5):1519–1527.

[20] Raichur, S., Wang, S.T., Chan, P.W., Li, Y., Ching, J., Chaurasia, B., et al., 2014. CerS2 haploinsufficiency inhibits beta-oxidation and confers susceptibility to diet-induced steatohepatitis and insulin resistance. Cell Metabolism 20(4):687–695.

[21] Scherer, P.E., Williams, S., Fogliano, M., Baldini, G., Lodish, H.F., 1995. A novel serum protein similar to C1q, produced exclusively in adipocytes. Journal of Biological Chemistry 270(45):26746–26749.

[22] Spiegel, S., Milstien, S., 2003. Sphingosine-1-phosphate: an enigmatic signalling lipid. Nature Reviews Molecular Cell Biology 4(5):397–407.

[23] Sun, K., Wernstedt Asterholm, I., Kusminski, C.M., Bueno, A.C., Wang, Z.V., Pollard, J.W., et al., 2012. Dichotomous effects of VEGF-A on adipose tissue dysfunction. Proceedings of the National Academy of Sciences 109(15): 5874–5879.

[24] Stefan, N., Machicao, F., Staiger, H., Machann, J., Schick, F., Tschritter, O., et al., 2005. Polymorphisms in the gene encoding adiponectin receptor 1 are associated with insulin resistance and high liver fat. Diabetologia 48(11): 2282–2291.

[25] Takabe, K., Paugh, S.W., Milstien, S., Spiegel, S., 2008. "Inside-out" signaling of sphingosine-1-phosphate: therapeutic targets. Pharmacological Reviews 60(2):181–195.

[26] Tsuchida, A., Yamauchi, T., Ito, Y., Hada, Y., Maki, T., Takekawa, S., et al., 2004. Insulin/Foxo1 pathway regulates expression levels of adiponectin receptors and adiponectin sensitivity. Journal of Biological Chemistry 279(29): 30817–30822.

[27] Turer, A.T., Browning, J.D., Ayers, C.R., Das, S.R., Khera, A., Vega, G.L., et al., 2012. Adiponectin as an independent predictor of the presence and degree of hepatic steatosis in the Dallas Heart Study. Journal of Clinical Endocrinology and Metabolism 97(6):E982–E986.

[28] Turpin, S.M., Nicholls, H.T., Willmes, D.M., Mourier, A., Brodesser, S., Wunderlich, C.M., et al., 2014. Obesity-induced CerS6-dependent C16:0 ceramide production promotes weight gain and glucose intolerance. Cell Metabolism 20(4):678–686.

[29] Villa, N.Y., Kupchak, B.R., Garitaonandia, I., Smith, J.L., Alonso, E., Alford, C., et al., 2009. Sphingolipids function as downstream effectors of a fungal PAQR. Molecular Pharmacology 75(4):866–875.

[30] Xia, J.Y., Holland, W.L., Kusminski, C.M., Sun, K., Sharma, A.X., Pearson, M.J., et al., 2015. Targeted induction of ceramide degradation reveals roles for ceramides in non alcoholic fatty liver disase and glucose metabolism in mice. Cell Metabolism 22(2):266–278.

[31] Xu, A., Wang, Y., Keshaw, H., Xu, L.Y., Lam, K.S., Cooper, G.J., 2003. The fat-derived hormone adiponectin alleviates alcoholic and nonalcoholic fatty liver diseases in mice. The Journal of Clinical Investigation 112(1):91–100.

[32] Xu, A., Wang, Y., Keshaw, H., Xu, L.Y., Lam, K.S.L., Cooper, G.J.S., 2003. The fat-derived hormone adiponectin alleviates alcoholic and nonalcoholic fatty liver diseases in mice. The Journal of Clinical Investigation 112(1):91–100.

[33] Yamauchi, T., Kamon, J., Ito, Y., Tsuchida, A., Yokomizo, T., Kita, S., et al., 2003. Cloning of adiponectin receptors that mediate antidiabetic metabolic effects. Nature 423(6941):762–769.

[34] Yamauchi, T., Kamon, J., Waki, H., Terauchi, Y., Kubota, N., Hara, K., et al., 2001. The fat-derived hormone adiponectin reverses insulin resistance associated with both lipoatrophy and obesity. Nature Medicine 7(8):941–946.

[35] Yamauchi, T., Nio, Y., Maki, T., Kobayashi, M., Takazawa, T., Iwabu, M., et al., 2007. Targeted disruption of AdipoR1 and AdipoR2 causes abrogation of adiponectin binding and metabolic actions. Nature Medicine 13(3):332–339.

[36] Yano, W., Kubota, N., Itoh, S., Kubota, T., Awazawa, M., Moroi, M., et al., 2008. Molecular mechanism of moderate insulin resistance in adiponectin-knockout mice. Endocrine Journal 55(3):515–522.

[37] Ye, R., Holland, W.L., Gordillo, R., Wang, M., Wang, Q.A., Shao, M., et al., 2014. Adiponectin is essential for lipid homeostasis and survival under insulin deficiency and promotes beta-cell regeneration. Elife 3.

 © 2017 Published by Elsevier GmbH. This is an open access article under the CC BY-NC-ND license (http://creativecommons.org/licenses/by-nc-nd/4.0/).